Egyptian Journal of Medical Human Genetics

RESEARCH

Open Access

Diagnostic biomarkers for ST-segment elevation myocardial infarction using RNA methylation regulators

Yeting Li[1†], Kai Ma[1†], Chuanxin Zhao[1], Nannan Li[1], Shanshan Li[1] and Man Zheng[1*]

Abstract

Aims Additional evidence has indicated a correlation between N6-methyladenosine (m6A) RNA methylation and cardiovascular disease. Nevertheless, the alterations in RNA methylation modification and the expression of numerous genes remains unclear. This study aimed to identify the role of m6A in ST-segment elevation myocardial infarction (STEMI).

Methods Two microarray datasets (GSE123342 and GSE59867) were downloaded from the GEO database. After merging the data and batch normalization, differentially expressed regulators were identified using the limma package. Subtyping consistency analysis was performed to group samples. The random forest algorithm and support vector machine were used to identify diagnostic biomarkers. Immune infiltration and inflammation levels among the subtypes were assessed using a single-sample gene set enrichment analysis.

Results A total of 15 key differential m6A regulators (RBM15B, ELAVL1, ALKBH5, METTL16, ZC3H13, RBM15, YTHDC1, YTHDC2, YTHDF3, HNRNPC, FMR1, LRPPRC, HNRNPA2B1, RBMX, FTO) were identified using the random forest classifier and were found to be highly correlated by PPI analysis. Two distinct RNA modification patterns (cluster A and B) were validated based on the expression levels of the 15 key m6A regulators. GO and KEGG annotations showed that immunity and inflammation pathways were enriched. Immune infiltration analysis revealed that cluster 2 had higher immune activation than cluster 1. Further analysis showed that cluster 2 had a higher inflammation level, with IL-4 and IL-33 showing differential expression ($p < 0.05$).

Conclusion A set of 15 m6A RNA methylation regulators could alter the STEMI microenvironment to improve risk stratification and clinical treatment.

Keywords Bioinformatics information, m6A RNA methylation, ST-segment elevation acute myocardial infarction, Immunology, Inflammation level

Introduction

Approximately 750,000 instances of ST-segment elevation myocardial infarction (STEMI) are identified each year in the USA [1]. This condition is frequently seen in emergency departments (ED). In 2000, 5% of all emergency department visits in the USA were due to chest pain, with 5–15% of those patients having an acute myocardial infarction.

Certain established biomarkers, including troponin and B-type natriuretic peptide, have been demonstrated

†Yeting Li and Kai Ma have contributed equally to this work and share first authorship.

*Correspondence:
Man Zheng
zhengman0815@163.com
[1] Department of Cardiology, Dongying People's Hospital (Dongying Hospital of Shandong Provincial Hospital Group), Dongying 257091, Shandong, China

to modestly improve the prognostic accuracy of clinical risk assessment for STEMI. The current diagnostic gold standard, the high-sensitivity troponin T assay (hsTnT), has this major limitation. Between sixty and seventy percent of healthy individuals residing in the community, especially older adults, exhibited detectable levels of hsTnT [2]. Hence, the identification of novel predictive biomarkers and potential therapeutic targets necessitates comprehensive data from biological systems, with RNA methylation markers emerging as promising candidates.

RNA methylation, specifically N6-methyladenosine (m6A) methylation, is a common epigenetic modification found in the 3' UTR and stop codon of mRNAs [3]. The m6A modification of mRNA plays a crucial role in various biological processes, including spermatogenesis, stem cell maintenance, circadian clock regulation, and cancer progression, by regulating different aspects of mRNA life [4] 5.

Nevertheless, there remains a dearth of knowledge regarding the modifications and role of RNA methylation in individuals suffering from ST-elevation myocardial infarction (STEMI). In order to address this knowledge gap, we undertook an integrative examination of the transcriptome and RNA methylome in peripheral blood samples obtained from STEMI patients, with the aim of elucidating variations in RNA methylation and their impact on gene expression during the progression of STEMI. Ultimately, our study identified potential biomarkers for diagnosis and targets for therapeutic intervention related to RNA methylation.

Materials and methods

Gene expression profile data collection

Two profiling datasets, GSE123342 ($n=22$ for healthy people and $n=170$ for STEMI patients) and GSE59867 ($n=44$ for healthy people and $n=390$ for STEIMI patients), were obtained from the NCBI Gene Expression Omnibus database (GEO, https://www.ncbi.nlm.nih.gov/geo/). The raw data underwent preprocessing through background correction and quantile normalization utilizing a robust multi-array average algorithm [6].

Selection of key m6A methylation regulators

A total of 26 m6A-related gene regulators, including 9 writers (METTL3, METTL14, METTL16, WTAP, VIRMA, ZC3H13, RBM15, RBM15B, and CBLL1), 15 readers (YTHDC1, YTHDC2, YTHDF1, YTHDF2, YTHDF3, HNRNPC, FMR1, LRPPRC, HNRNPA2B1, IGFBP1, IGFBP2, IGFBP3, RBMX, ELAVL1, and IGF2BP1), and 2 erasers (FTO and ALKBH5), were analyzed in this study. We merged and batch-normalized the GSE123342 and GSE59867 databases using the Perl 5.32.1001 and R packages (sva and limma 3.40.6). The Limma package was used to identify correlations between the m6A RNA methylation regulators. The comprehensive gene expression matrix was obtained after merging the GSE123342 dataset and the GSE59887 dataset and batch normalization. Statistical significance was defined as $p<0.05$. Heatmaps and box plots were construed to determine differentially expressed genes, which were being highlighted as DEGs. Finally, the chromosomal locations of the differentially expressed m6A regulators were characterized with Circos software.

Construction and verification of the nomogram

The "rms" package in R software was used to construct predictive nomograms based on the expression values of six key m6A regulators. The calibration curve assessed the predictive power of the nomogram.

Consensus clustering for STEMI samples

Classification of STEMI samples based on genes associated with m6a methylation by the "Consensus Cluster Plus" package in the R software [7]. The ideal cluster number was identified using the consensus matrix (CM) and cumulative distribution function (CDF) curves of the consensus score [8]. We also performed principal component analysis (PCA) with different clusters.

Assessment of biological variables among various differently expressed gene of different cluster with STEMI patients

Gene Ontology (GO) analysis is a standard method for conducting large-scale functional enrichment studies covering biological processes, molecular functions, and cellular components [9]. Kyoto Encyclopedia of Genes and Genome (KEGG) is a widely used database for storing information on genomes, biological pathways, diseases, and pharmaceuticals [9]. GO annotation analysis and KEGG pathway enrichment analysis of the differentially expressed genes were performed using the R's clusterProfiler package [9], and $p<0.05$ for false discovery rate was considered statistically significant.

Protein–protein interaction (PPI) network construction and hub genes identification

A PPI network was constructed using the online STRING database (STRING, version 11.5; https://cn.string-db.org) to predict interactive relationships between differentially expressed genes. Cytoscape 3.8.2 was employed for PPI network visualization and hub gene analysis.

Immunity and inflammation infiltration analysis

ssGSEA is an extension of genomic enrichment analysis (GSEA) to determine the intensity of immune cell infiltration. The tool can be used to define enrichment scores

that provide a representation of the absolute level of enrichment of genomes in each sample in a given dataset. Using the "GSVA" R package, we performed ssGSEA to examine differences in immune cell infiltration between the two groups and determine whether there was any correlation between the two subtypes [10].

Results

Screening and identification of differentially expressed m6A regulators

The available numerical expression values of patients with STEMI and healthy controls from GSE123342 and GSE59867 after sample merging and batch normalization were analyzed to identify differentially expressed m6A regulators. As shown in the box plot (Fig. 1A) and heatmap plot (Fig. 1B), there were 3 upregulated (RBM15B, ELAVL1, ALKBH5) and 12 downregulated (METTL16, ZC3H13, RBM15, YTHDC1, YTHDC2, YTHDF3, HNRNPC, FMR1, LRPPRC, HNRNPA2B1, RBMX, FTO) m6A regulators in STEMI patients compared with healthy controls. The chromosomal location of a gene can provide information about its developmental history, including gene replication patterns and gene reproduction events[11]. A total of 26 m6A-related genes were allocated on 15 chromosomes, with the maximum number of genes located on chromosome 17 ($n=2$) and X ($n=2$) (Fig. 1C). The PPI network was used to elucidate gene–gene interaction networks. The results showed that the 15 differentially expressed m6A regulators had a higher number of differentially expressed m6A regulators (Fig. 1D).

Random forest screening and assessment of a nomogram model

The residual in random forest (RF) is smaller than that in the SVM; therefore, the RF was validated for later research (Fig. 2A). 15 key m6A regulators with significance > 2 was identified for follow-up analysis (Fig. 2B). Predictive nomograms were constructed on the basis of

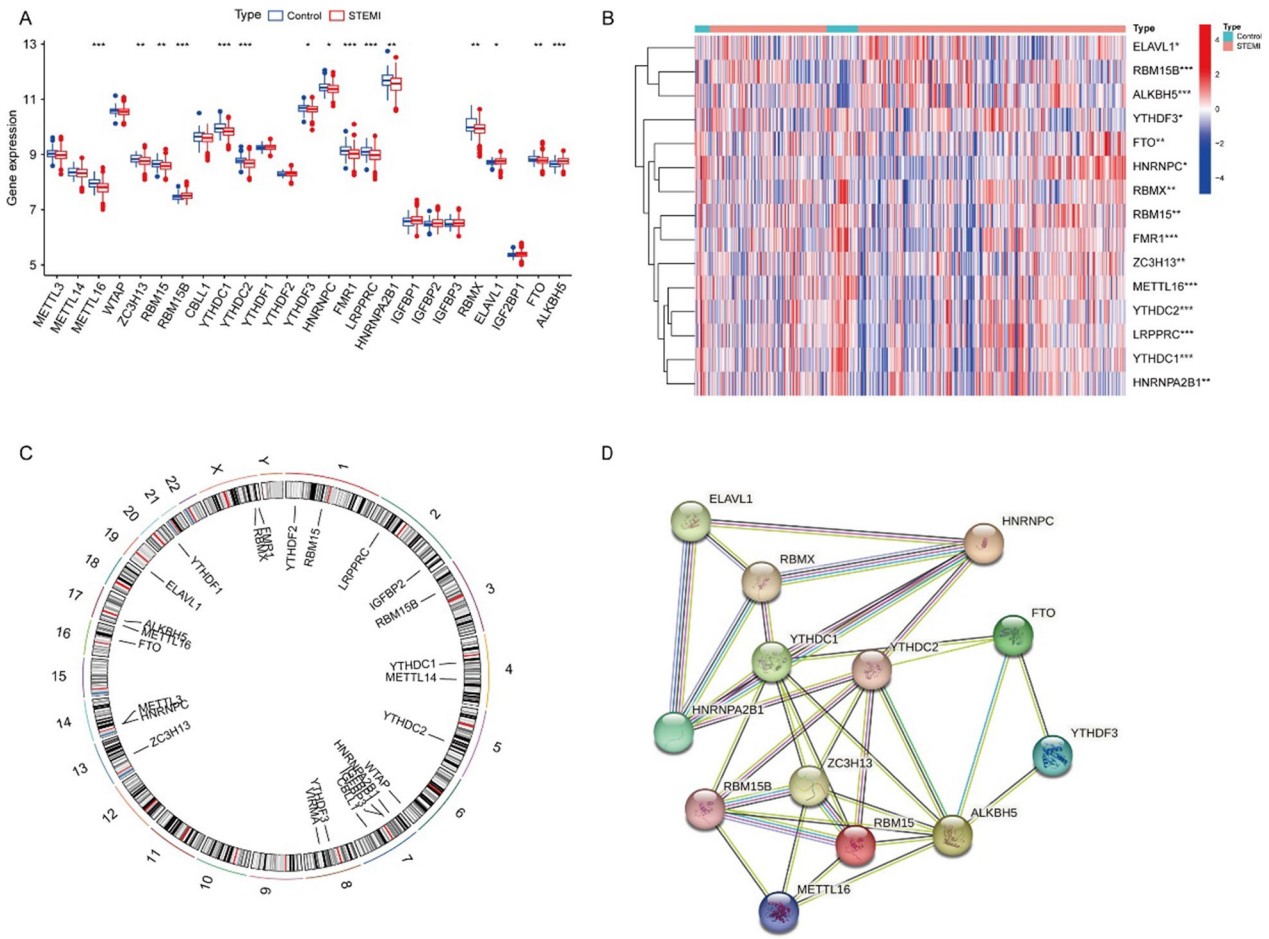

Fig. 1 Screening and identification of differentially expressed m6A-related genes. **A** Box plot of differentially expressed m6A regulators. **B** Heatmap of differentially expressed m6A regulators. **C** Circos plot showing the location of genes in 22 chromosomes. **D** Protein–protein interaction networks. *$p<0.05$, **$p<0.01$, ***$p<0.001$

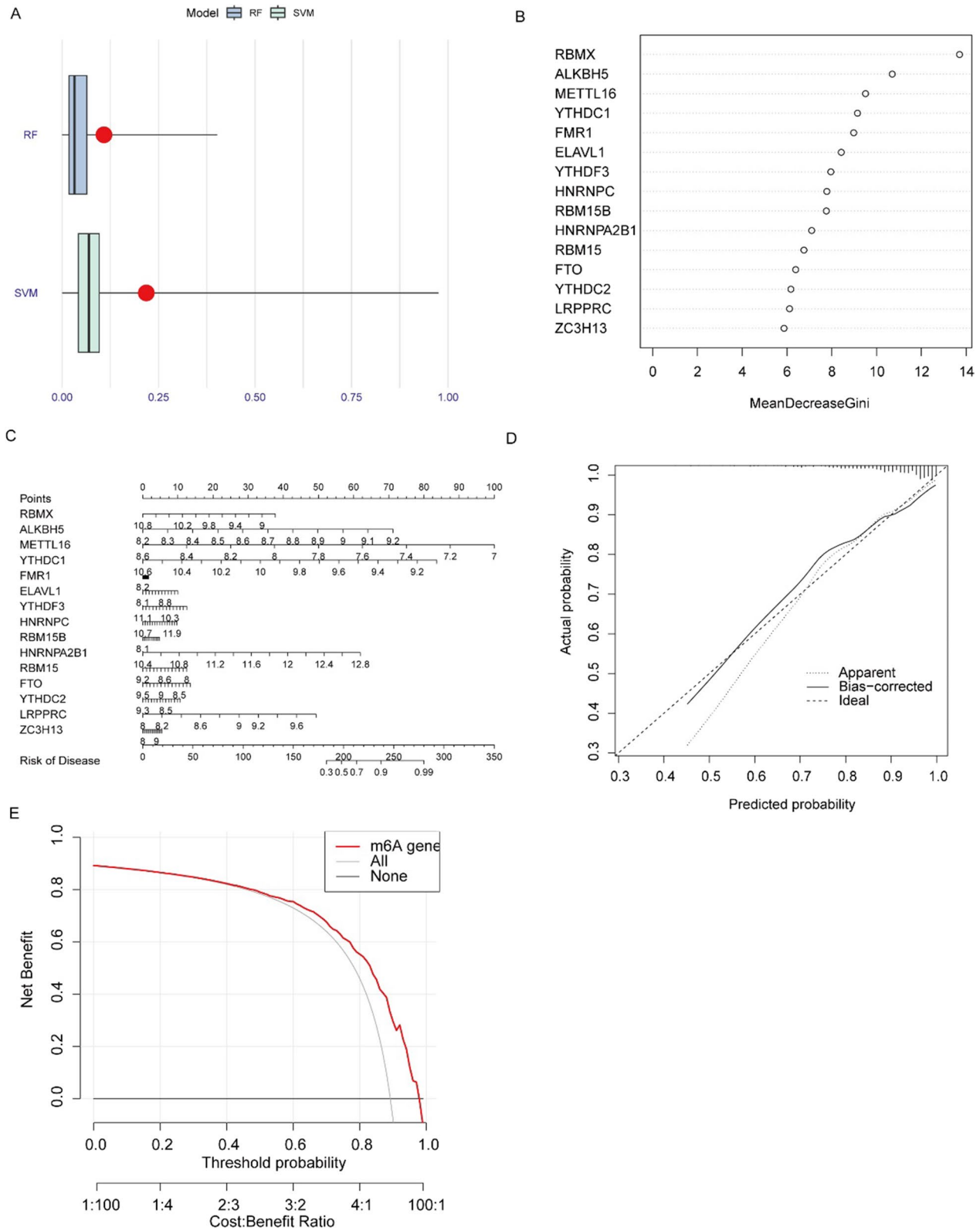

Fig. 2 Random forest screening and assessment of a nomogram model. **A** Boxplots of residuals. **B** Random forest screening and assessment of a nomogram model. **C** The nomogram of the model. **D** Calibration curve can assess the utility of models for decision making. The closer the solid and dotted lines are, the higher the accuracy of the model's predictions **E** Decision curve analysis (DCA) of the nomogram. The solid line represents the performance of the nomogram, of which a closer fit to the diagonal dotted line represents a better prediction

expressions with significance greater than 2 (Fig. 2C). According to the calibration curves, the error between the predicted STEMI risk and the actual STEMI risk is very low, indicating the nomogram model is very accurate (Fig. 2D). Decision curve analysis (DCA) showed that the Kaplan-Meier curve was higher than the gray line. The findings indicated that the nomogram continues to demonstrate significant clinical utility in forecasting the morbidity of patients with STEMI (Fig. 2E).

Validation STEMI patient subgroup based on differently expressed m6A regulators

A consensus clustering analysis was conducted utilizing differentially expressed m6A genes in order to delineate unique RNA methylation prognostic molecular subtypes of STEMI. According to the CDF and CDF delta area curves, the area under the CDF curve was stable across 2 categories (Fig. 3A, B). The color-coded heat map and PCA results are shown in Fig. 3C. This represents

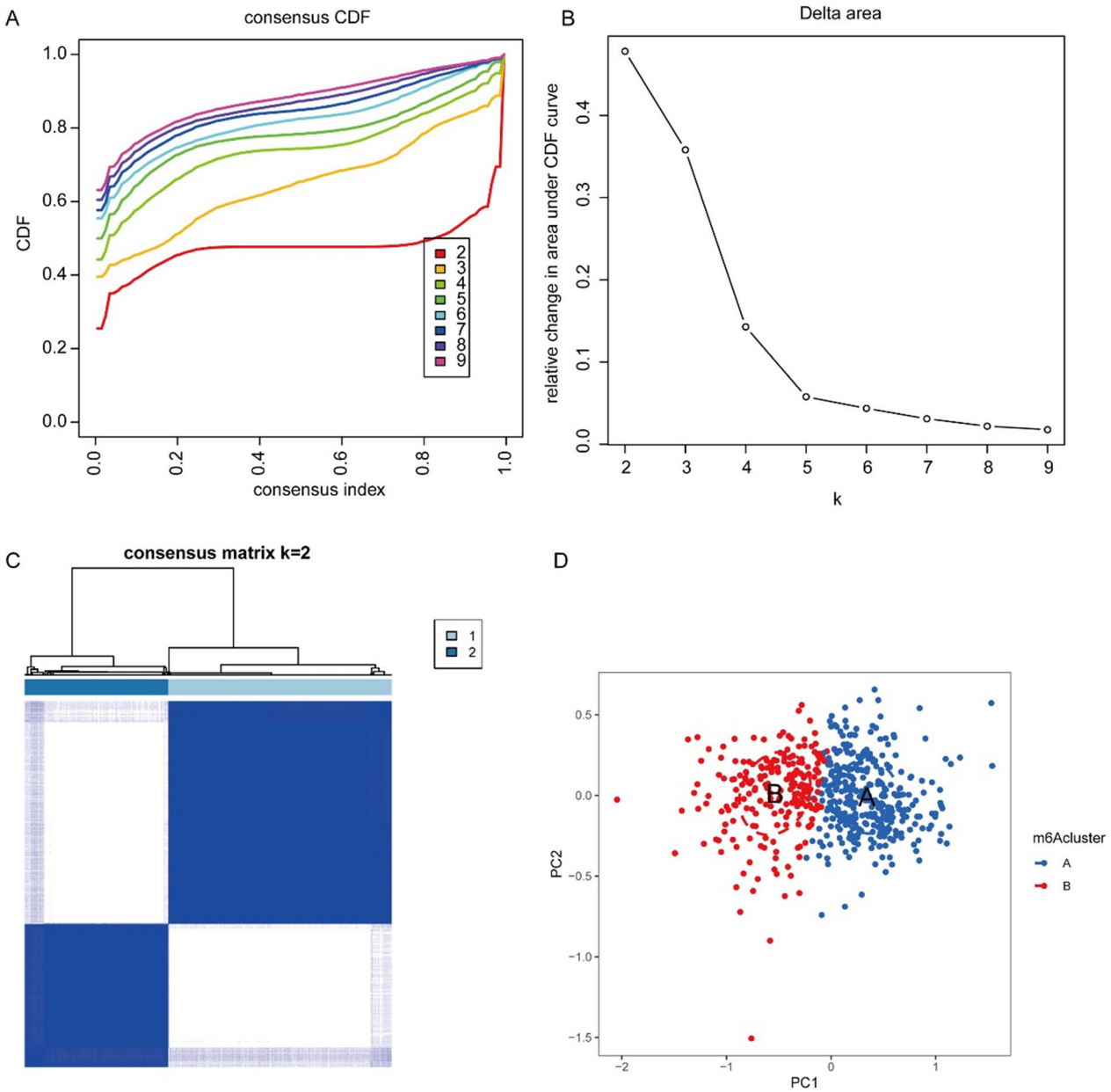

Fig. 3 Validation STEMI patient subgroup based on differently expressed m6A regulator. **A** CDF curve of samples in the STEMI cohort for k = 2–9. **B** Relative change in the area under the CDF curve for k = 2–9. **C** Sample clustering heatmap when consumption k = 2. **D** Principal component analysis of the transcriptome profiles cluster A and cluster B, showing a remarkable difference in the transcriptome between different modification patterns

consensus ($k=2$), which displays a clear distribution between cluster A and cluster B (Fig. 3D).

Biological GO pathway and immune infiltration level among different cluster with STEMI patients

Subsequently, an analysis was conducted to investigate the involvement of differentially expressed genes (DEGs) in biologically significant functions within subgroups categorized based on m6A-related genes. GO analysis revealed enrichment of DEGs in pathways associated with regulating immune responses (Fig. 4A and B). Based on the findings of the functional analysis, we conducted a more in-depth investigation into the correlation of immune cell infiltration levels within the two clusters. Our analysis revealed that a majority of immune cells (19/23) exhibited varying degrees of infiltration in the distinct clusters (Fig. 4C). Compared to cluster A, cluster B exhibited elevated levels of immune cell infiltration, particularly dendritic cells, natural killer cells, macrophages, mast cells, and neutrophils ($p<0.001$). Furthermore, an analysis was conducted on the correlation between 15 differentially expressed m6A regulators and 23 immune cells. It was found that a majority of m6A-related genes exhibit a strong correlation with immune cell infiltration, particularly LRPPRC and HNRNPA2B1 (Fig. 4D).

Biological KEGG pathway and inflammation level among different cluster with STEMI patients

The analysis of KEGG data revealed that DEGs predominantly enriched two pathways: the immune-related pathway, such as B cell receptor signaling, and the inflammation reaction pathway, such as TNF, IL-17, and other pathways (Fig. 5A). Following the analysis of KEGG results, we conducted a comprehensive evaluation of the association between the differentially expressed genes

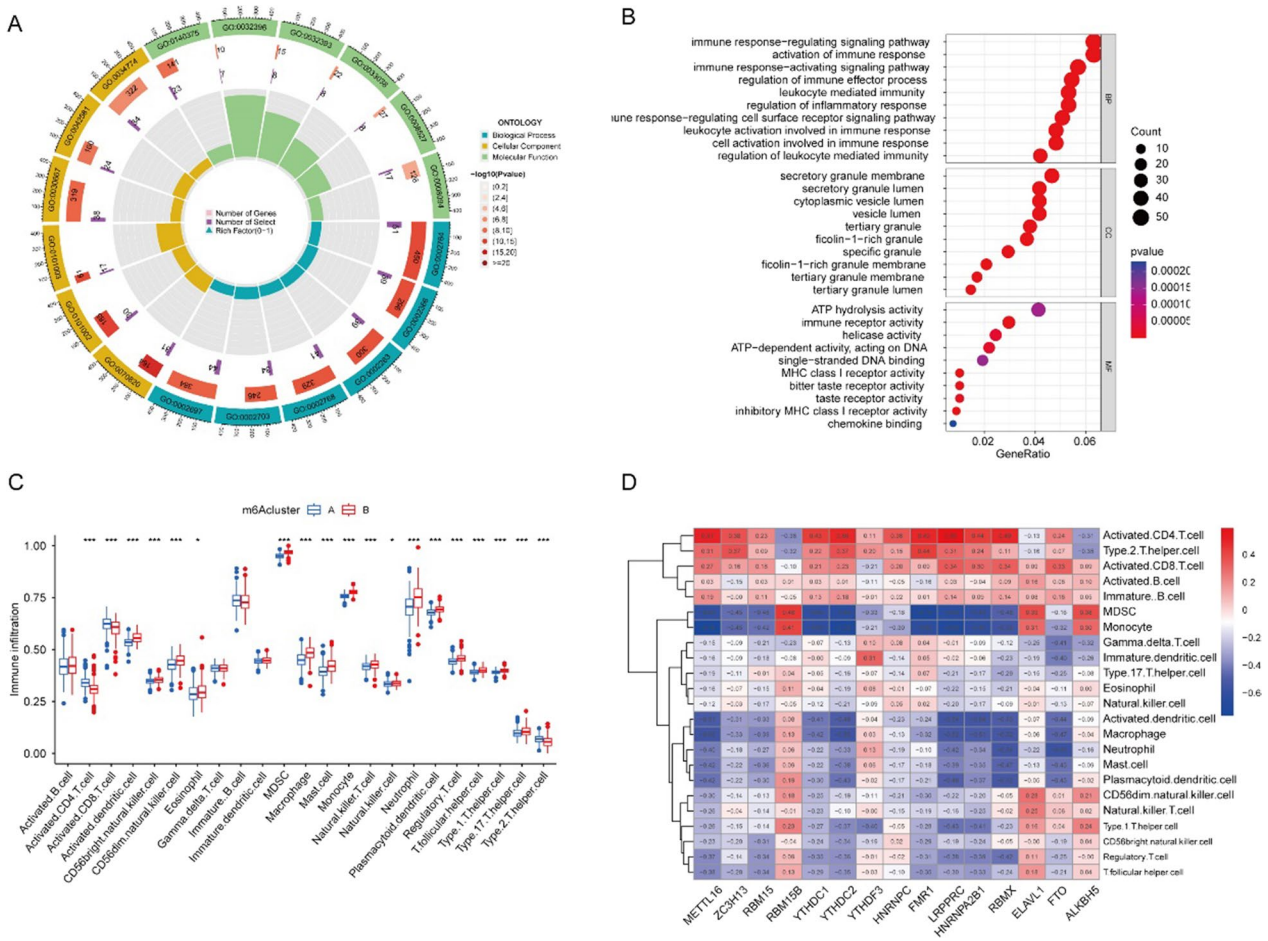

Fig. 4 Biological GO pathway and immune infiltration level among different cluster with STEMI patients. **A**, **B** Gene Ontology (GO) functional analysis. **C** Comparison of immunocyte abundance in the 2 clusters. **D** The heatmap between differently expressed m6A gene and immune cell. *$p<0.05$, ***$p<0.001$

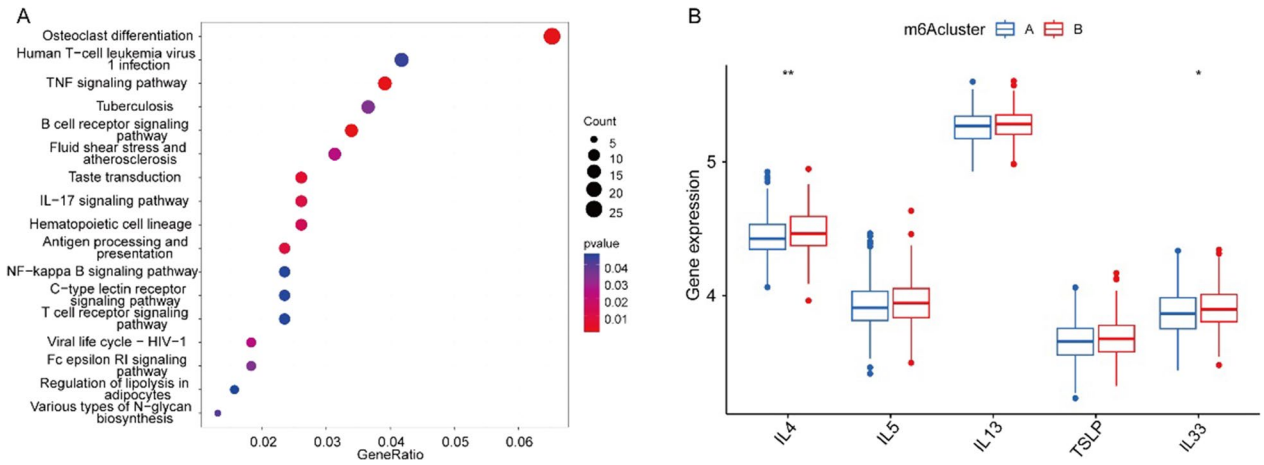

Fig. 5 Biological KEGG pathway and inflammation level among different cluster with STEMI patients. **A** Kyoto Encyclopedia of Genes and Genomes (KEGG) pathway enrichment analysis. **B** Boxplots of inflammation levels. *$p < 0.05$, **$p < 0.01$

and levels of inflammation. It was observed that the expression levels of IL-4 and IL-33 were significantly elevated in cluster B compared to cluster A (Fig. 5B). These results confirm that inflammation plays an important role in methylation, especially IL-4 and IL-33.

Discussion

In summary, this novel study synthesized RNA methylation expression datasets from STEMI patients to identify epigenetic alterations associated with STEMI. Initially, our analysis identified three upregulated and twelve downregulated differentially expressed m6A regulators in correlation with the progression of STEMI disease. Subsequently, consensus clustering analysis demonstrated the potential classification of patients into two distinct groups based on the expression levels of m6A-related regulators. Changes in numerous methylation modification sites are observed during this stage, impacting the expression of genes downstream. It is hypothesized that m6A modification patterns significantly influence the development of the STEMI immune microenvironment. Notably, inflammatory factors IL-4 and IL-33 have been implicated in STEMI through an m6A modification pattern.

Lack of sensitivity and specificity are major limitations in the assessment of STEMI. Despite its crucial role in the evaluation of STEMI patients, there has been a consistent decrease in the sensitivity of cardiac troponin concentration in systemic venous blood; novel polygenic diagnostic biomarkers have the potential to address this limitation. In our study, a random forest algorithm was employed to identify 15 diagnostic markers linked to m6A, demonstrating high stability and accuracy in diagnosing STEMI. Cardiomyocytes subjected to hypoxia/reoxygenation (H/R) exhibited heightened autophagic activity and reduced apoptosis following silencing of METTL3 [12]. Arcidiacono et al. observed an increase in the fluorescence intensity of the METTL16 protein in α-actinin positive cells in the cardiomyocytes group compared to the control group [13]. Significantly, a novel diagnostic nomogram was developed and validated for risk prediction in patients with STEMI utilizing a panel of 15 biomarkers. This approach facilitated improved categorization of STEMI patients.

Many biological processes observed in STEMI patients involve inflammation and immune cell infiltration. Based on GO enrichment analysis, two clusters of STEMI were shown to have differentially expressed genes related to immune response-regulating and immune response-activating signaling pathways. Based on KEGG enrichment analysis, two clusters of STEMI differentially expressed genes were associated with human T-cell leukemia virus 1 (HTLV-1) infection and TNF signaling. HTLV-1, first diagnosed in 1980 in a patient with cutaneous lymphoma, can cause inflammatory diseases [14]. Another study reported that HTLV-1 causes atherosclerosis by inducing inflammation [15]. Emerging research indicates that dysregulation of immune-inflammatory pathways, including IL-4 and TNF, play a significant role in the pathogenesis of various diseases, such as panic disorder and kidney transplant rejection [16–18]. There is a lack of existing data regarding immune-inflammatory pathway methylation in individuals with ST-segment elevation myocardial infarction (STEMI). Our research represents the inaugural investigation into the potential promotion of methylation through elevated levels of interleukin-4 (IL-4) and interleukin-33 (IL-33), leading to the onset of STEMI. Significantly, our findings propose that the

targeting of IL-4 and IL-33 may offer protective benefits against methylation in STEMI patients.

In recent years, several important molecules associated with immune cells have been discovered as potential novel biomarkers for application in disease diagnosis and prognosis [19]. Li et al. [20] discovered that the molecular markers PPBP, CXCL12, and CCL4 were associated with immune cell infiltration in valvular atrial fibrillation. RBMX is involved in alternative splicing and was initially recognized as a constituent of the spliceosome. More recently, RBMX has been demonstrated to be involved in DNA damage repair, sister chromatid cohesion, and the assembly of higher-order ribonucleoprotein complexes to maintain genomic stability [21]. The role of RBMX in cardiovascular diseases has yet to be definitively established. Our research findings indicate that key immune-related genes are involved in the pathogenesis of STEMI, as identified through heat map analysis. The dark blue module depicted in the box plot demonstrates a strong association with infiltrating immune cells, indicating a high negative correlation between LRPPRC and HNRNPA2B1 with various immune cell types, including dendritic cells, macrophages, neutrophils, and mast cells. RBMX expression was lower in m6A cluster A compared to cluster B, indicating its potential role in STEMI pathogenesis and suggesting new treatment targets.

Our study has some limitations primarily due to potential misunderstandings and biases that may have arisen during the unsupervised clustering process, attributable to the restricted sample size. Consequently, further research utilizing larger sample sizes is imperative. Furthermore, substantial prospective studies with a meticulous follow-up methodology are essential to confirm the clinical viability of the suggested biomarkers.

Conclusion

In conclusion, our thorough analysis of m6A modifications has revealed their significant impact on the intricate immune infiltration patterns observed in STEMI. Furthermore, through unsupervised clustering, we have identified two distinct subtypes of m6A modifications that have the potential to differentiate between varying degrees of STEMI severity. Immunophenotyping STEMI patients may therefore facilitate the development of more targeted immunotherapy approaches for individuals exhibiting pronounced immune responses. Additionally, the modulation of m6A modifications has been shown to influence the expression of inflammation-related genes such as IL-4 and IL-33, presenting a promising new avenue for therapeutic intervention in STEMI.

Acknowledgements
Funding sources are not available.

Author contributions
YL and KM conducted statistical analysis and wrote the manuscript, while CZ, NL, and SL contributed ideas and constructive suggestions for the research. MZ oversaw the design and review of the study. The study did not require approval from an ethical review board.

Funding
This work was supported by research grants from Shandong Province Medical and Health Technology Development Plan Project (2019WS040) and Shandong Traditional Chinese Medicine Technology Project (2021Q039).

Availability of data and materials
The data that support the findings of this study are available from the corresponding author, upon reasonable request.

Declarations

Ethical approval and consent to participate
Not applicable.

Consent for publication
Not applicable.

Competing interests
There is no potential conflict of interest.

Received: 9 April 2024 Accepted: 3 May 2024
Published online: 28 May 2024

References

1. Abe T, Olanipekun T, Adedinsewo D et al (2023) Trends and outcomes of ST-segment-elevation myocardial infarction among young women in the United States. J Am Heart Assoc 12(5):e26811
2. Saunders JT, Nambi V, de Lemos JA et al (2011) Cardiac troponin T measured by a highly sensitive assay predicts coronary heart disease, heart failure, and mortality in the Atherosclerosis Risk in Communities Study. Circulation 123(13):1367–1376
3. Roignant JY, Soller M (2017) m(6)A in mRNA: An ancient mechanism for fine-tuning gene expression. Trends Genet 33(6):380–390
4. Lin Z, Hsu PJ, Xing X et al (2017) Mettl3-/Mettl14-mediated mRNA N(6)-methyladenosine modulates murine spermatogenesis. Cell Res 27(10):1216–1230
5. Zheng Q, Hou J, Zhou Y et al (2017) The RNA helicase DDX46 inhibits innate immunity by entrapping m(6)A-demethylated antiviral transcripts in the nucleus. Nat Immunol 18(10):1094–1103
6. Irizarry RA, Hobbs B, Collin F et al (2003) Exploration, normalization, and summaries of high density oligonucleotide array probe level data. Biostatistics 4(2):249–264
7. Wang B, Tong F, Zhai C et al (2021) Derivation and comprehensive analysis of aging patterns in patients with bladder cancer. Dis Markers 2021:3385058
8. Zhou Q, Yan X, Liu W et al (2020) Three immune-associated subtypes of diffuse glioma differ in immune infiltration, immune checkpoint molecules, and prognosis. Front Oncol 10:586019
9. Wilkerson MD, Hayes DN (2010) ConsensusClusterPlus: a class discovery tool with confidence assessments and item tracking. Bioinformatics 26(12):1572–1573
10. Hanzelmann S, Castelo R, Guinney J (2013) GSVA: gene set variation analysis for microarray and RNA-seq data. BMC Bioinformatics 14:7
11. Holland PW, Booth HA, Bruford EA (2007) Classification and nomenclature of all human homeobox genes. BMC Biol 5:47
12. Song H, Feng X, Zhang H et al (2019) METTL3 and ALKBH5 oppositely regulate m(6)A modification of TFEB mRNA, which dictates the fate of hypoxia/reoxygenation-treated cardiomyocytes. Autophagy 15(8):1419–1437

13. Arcidiacono OA, Krejci J, Bartova E (2020) The distinct function and localization of METTL3/METTL14 and METTL16 enzymes in cardiomyocytes. Int J Mol Sci 21:8139
14. Poiesz BJ, Ruscetti FW, Gazdar AF et al (1980) Detection and isolation of type C retrovirus particles from fresh and cultured lymphocytes of a patient with cutaneous T-cell lymphoma. Proc Natl Acad Sci U S A 77(12):7415–7419
15. Takeoka H, Sagara Y, Ksashiwagi S et al (2021) Human T-cell leukemia virus type 1 infection is a risk factor for atherosclerosis. J Clin Med Res 13(3):164–169
16. Zou Z, Huang Y, Wang J et al (2020) DNA methylation of IL-4 gene and the association with childhood trauma in panic disorder. Psychiatry Res 293:113385
17. Soyoz M, Pehlivan M, Tatar E et al (2021) Consideration of IL-2, IFN-gamma and IL-4 expression and methylation levels in CD4+ T cells as a predictor of rejection in kidney transplant. Transpl Immunol 68:101414
18. Guo X, Zhu Y, Sun Y et al (2022) IL-6 accelerates renal fibrosis after acute kidney injury via DNMT1-dependent FOXO3a methylation and activation of Wnt/beta-catenin pathway. Int Immunopharmacol 109:108746
19. Qiu Y, Li H, Xie J et al (2021) Identification of ABCC5 among ATP-binding cassette transporter family as a new biomarker for hepatocellular carcinoma based on bioinformatics analysis. Int J Gen Med 14:7235–7246
20. Li S, Jiang Z, Chao X et al (2021) Identification of key immune-related genes and immune infiltration in atrial fibrillation with valvular heart disease based on bioinformatics analysis. J Thorac Dis 13(3):1785–1798
21. Zheng T, Zhou H, Li X et al (2020) RBMX is required for activation of ATR on repetitive DNAs to maintain genome stability[J]. Cell Death Differ 27(11):3162–3176

Publisher's Note